Research Article

A. Jacas-Rodríguez*, P. Rodríguez-Pascual, D. Franco-Manzano, L. Contreras, C. Polop, and M. A. Rodriguez

Mixed Matrix Membranes prepared from polysulfone and Linde Type A zeolite

https://doi.org/10.1515/secm-2020-0022
Received Mar 09, 2020; accepted Jun 08, 2020

Abstract: This work focuses on dip coating and further phase inversion prepared polysulfone/LTA zeolite mixed matrix membranes (*MMMs*). The Linde Type A (LTA) zeolite synthesized under hydrothermal conditions by the organic free method was introduced as fillers at 10 and 20 wt.% loadings into the polysulfone polymer matrix to obtain *MMMs*. The x-ray diffraction (XRD) and scanning electron microscopy (SEM) analysis indicated that the as-synthesized LTA zeolite samples were crystalline and mainly composed of crystal of predominantly cubic shape. Textural characterisation using Ar adsorption/desorption data of LTA zeolite shown the existence of mesoporous. Atomic force microscopy (AFM) in combination with the SEM characterised the membrane morphology and the dispersion of zeolite fillers. The effect of the zeolite loading on the performance of the *MMMs* was analysed. It points out that N_2 permeability was increased with the increment of zeolite filler, also the high membranes permeability and the weak dependence upon transmembrane pressure and therefore its high selectivity. The average membrane thickness was 150 μm.

Keywords: Zeolite, hydrothermal synthesis, adsorption, polysulfone, permeation

***Corresponding Author: A. Jacas-Rodrıguez:** Instituto de Ciencia de Materiales de Madrid. (CSIC). Cantoblanco 28049. Madrid, Spain; Universidad Nacional de Educación a Distancia (UNED), Madrid. Spain; Email: ajacas@icmm.csic.es;
ORCID ID https://orcid.org/0000-0002-6646-1315
P. Rodrıguez-Pascual: Instituto de Ciencia de Materiales de Madrid. (CSIC). Cantoblanco 28049. Madrid, Spain
D. Franco-Manzano, L. Contreras, M. A. Rodriguez: Instituto de Cerámica y Vidrio (ICV-CSIC). Cantoblanco 28049. Madrid. Spain
C. Polop: Departamento de Física de la Materia Condensada and Condensed Matter Physics Center (IFIMAC), Universidad Autónoma de Madrid, 28049 Madrid, Spain

1 Introduction

The first synthesis of LTA zeolite took place in 1956 at Union Carbide Labs by hydrothermal synthesis under the efforts of Breck and co-workers [1]. Since this challenge and before, many other zeolite structures have been obtained by different methods, but well-known zeolites as the LTA structure keep the interest under new perspectives due to its different fields of application on the commercial scale and in terms of scientific research [2].

Many are the essential properties of zeolite membranes, among them, highly ordered crystalline structure, thermal stability that makes the membranes useful at high-temperature operations, chemical resistance, controlled host-sorbate interaction and uniform molecular size pores. Taking into consideration all of them, different studies have been carried out on the preparation and characterization of zeolite membranes during the last thirty years [3–5].

In general, preparation of membranes with zeolite use one of the two following routes [6]:

(a) Crystallization of zeolite film by growing the zeolite layer on porous support like ceramic, metal or glass or self-supported membranes by direct grows without any support or growing the zeolite layer over temporary support.
(b) Use of zeolite crystal previously synthesised as inorganic fillers to produce zeolite-filled membranes by embedding zeolite crystal into different kinds of matrices.

However, zeolite membranes is still a challenge nowadays because their fragile structures make the development of large-scale inorganic membranes hard, especially to produce reliable defect-free membrane and cost-effective fabrication processes [7]. For this reason, despite the results in the development of zeolite membranes, only a few industrial applications are considered nowadays [4].

The first synthetic membranes from organic nature were developed with cellulose and its derivative products, but their performance under the chemical environment or temperature was too low [8]. The development of new or-

ganic membranes using polymers as polyamide, polyacrylonitrile, and others with better resistance to chemical environment and better glass transition temperatures (T_g) in comparison with cellulose membranes have allowed their inclusion in new processes for polymeric membranes never seen. Other polymers as polysulfone, polyester sulfone, etc., in addition to chemical stability and T_g, compared to those before, have excellent mechanical properties.

The possibility of incorporating polymers and inorganic components into a material has been explored since the early industrialization of the polymers. Insertion of inorganic materials as fillers in the system could improve optical and mechanical properties [9]. The development of inorganic chemistry in recent decades and the introduction of the concept of "organic-inorganic hybrid materials" combined with multi-functionalization [10] has allowed the development of custom products. In these products, the coexistence on the nanoscale of organic and inorganic phases makes them candidates for applications such as nonlinear optics, electronics, sensors, and catalysts [11].

The first research about mixed matrix membranes (*MMMs*) was developed around 1970 with the addition of 5A zeolite as fillers into the polymeric matrix showing the best gas separation performance in comparison to organic membranes made by polymer as a single-phase [12]. Synthetic zeolite as the dispersed phase is the most inorganic materials used as fillers into the *MMMs*, improving the possibilities of this system for gas separations [11], but only the membrane modification processes allow to eliminate or reduce the compatibility lack in the interphase between zeolite particles and polymer chains [13].

The development of organic-inorganic membranes presents improvements in the properties of permeability, selectivity as well as their thermal and mechanical properties. Due to the differences between the properties of the polymer and the inorganic phases, and the strong tendency of nanofillers to form aggregates, it is challenging to prepare *MMMs*. Because of the weak adhesion between the polymer and the inorganic particles, this type of membranes usually presents a variety of defects in the polymer-particle interphase [14–16].

The main objective has been to prepare mixed matrix membranes, where LTA zeolite was used as a dispersed phase in a polysulfone matrix. The physical and chemical properties of the zeolite and the resultant membranes were studied using different characterisation techniques, including the analysis of the influence of zeolite content on the *MMMs* and the final membrane performance under 1-6 bar N_2 transmembrane pressure difference.

2 Experimental details

2.1 Materials

All the compounds were from Sigma-Aldrich in ACS reagent grade: sodium silicate solution ($Na_2SiO_3 \cdot 5H_2O$), sodium hydroxide (NaOH 97%), sodium aluminate ($Na_2Al_2O_4 \cdot 3H_2O$), 1-methyl-2 pyrrolidone as solvent (purity > 99.5%), polysulfone (average Mw ~35,000; melt index of about 6.5 g/10 min) and deionised water.

2.2 LTA zeolite synthesis

Preparation of the LTA zeolite powders by a direct hydrothermal cycle was done following the best synthesis conditions from previous optimisation studies on the effect of the reaction times and its significant results on the zeolite crystal structures [17]. Briefly, the starting aluminosilicate gel molar composition 34 Na_2O:Al_2O_3:3SiO_2:462 H_2O was obtained by mixing an aluminate solution with a silicate solution under magnetic stirring. The aluminate solution was prepared by dissolving 4.36 g of sodium aluminate in 80 g of deionised water at 55°C up to apparent total solubility and then the addition of 24 g of sodium hydroxide, all under vigorous magnetic stirring. The silicate solution was obtained by mixing 12.76 g of sodium silicate in 80 g of deionised water at 55°C, followed by the addition of 24 g of sodium hydroxide until a clear solution, all under vigorous magnetic stirring. Finally, mixing both previous solutions under vigorous magnetic stirring at 85°C.

The final light white aluminosilicate hydrogel was stirred for more 10 min at this temperature before being transferred to a teflon coated wall stainless steel reactor and then, placed in an oven at a temperature of 100°C. The synthesis was carried out by static hydrothermal method at autogenous pressure at the mentioned temperature with a fixed crystallisation time of 75 min. Once the crystallisation time was over, the reactor was cooled and the as-synthesised product recovered by filtration, washed many times with deionised water up to constant pH of wash waters and then dried in air at 60°C for 12 h.

2.3 Mixed matrix membrane preparation

Two different samples of polymer/zeolite composite membranes were prepared by the phase inversion technique, both with the same solvent and polysulfone matrix but different amounts of zeolite fillers. Similar conditions

(normal pressure and ambient temperature) were used at this step to avoid any external influence on the mechanical properties and performance.

Five steps were considered during the preparation of the *MMMs*:

(a) Preparation of a fraction of dispersed zeolite suspension in the solvent: Dispersed zeolite powders were sieved through-out a 150 µm sieve and subject to a suspension procedure in proportions of 10 % and 20 % by weight relative to 60 cm^3 of the organic solvent methyl-2-pyrrolidone. The zeolite powders were first stirred in the solvent and then ultra-sonicated in a 50W ultrasonic bath for 15 min interval.
(b) Addition and dissolution of polysulfone polymer in the proportion of 15 weight per cent concerning solvent into the zeolite suspension under magnetic stirring at 300 rpm for 6 hours at room temperature.
(c) The dispersed polymer/zeolite suspension was dip-coated on the surface of the glass plate by immersing the glass plate inside the suspension at a constant speed of 0.03 m/s, retention by 5s, and extraction at the same speed.
(d) Application of the phase inversion technique to get the membranes by immersing the dip-coated glass plates into deionised water and separating the condensed film.
(e) Solvent removal by evaporation in the air at 60°C for 24 h.

2.4 Characterisation

The LTA zeolite powders were characterized by XRD using an Advance Bruker D8 diffractometer (CuKα radiation at 40KV and 30mA, 2θ range from 5° to 50°, step size of 0.05, room temperature), for confirming the final phases developed during the present study as well as the degree of zeolite powders crystallinity. Scanning electron microscopy (SEM, HITACHI S-4700) was used to analyse morphology aspects of this structure. Thermogravimetry analysis was performed using STA 409 (Netzsch, Deutschland), designed for simultaneous TGA-DTA measurements at a heating rate of 5°C·min^{-1} under N_2 atmosphere to observe the zeolite behaviour as a function of temperature and its thermal properties. Fourier-transform infrared spectroscopy (FTIR, Bruker Optics IFS 66V/S Vacuum FT-IR) with a resolution of 2cm^{-1} over a wavenumber range of 4000 to 400 cm^{-1} in transmission setup and 64 scans was used to study the location of the different vibrational bands of the zeolite as the source of specific structural information. The samples were prepared by the KBr pellets. Finally, gas adsorption-desorption isotherm (Micromeritics ASAP 2020) was used to measure the specific surface area as well as other parameters using N_2 and Ar as the adsorbate. Before isotherms measurements, the samples were degassed at 10^{-1} Pa to be activated at 350°C for a minimum of 12h (ISO Standard 9277:2010-09).

The *MMMs* were characterised by SEM (HITACHI S-4700) and by atomic force microscopy (AFM). For the SEM studies, the *MMMs* were torn at room temperature to check their cross-section. Samples were gold-sputtered before testing. The AFM experiments were performed with a commercial AFM (Nanotec Electrónica S.L.) in a dry N_2(g) atmosphere [18]. Under these conditions, the environmental humidity was held below 10% to avoid capillary forces. Si cantilevers (PPP-NCHR Nanosensors) with a force constant K = 40N/m, tip radius R_{tip} = 10 nm and resonance frequency f_0 = 300 kHz were used. Topographic images were acquired in tapping mode with a scanning rate between 0.5 and 1 Hz and analysed by the WSxM software [18]. Besides, N_2 permeation using a lab experimental setup [19] where the mass flow controller was used to control the N_2 gas to the membrane. Finally, the measurements of membrane thickness using a digital micrometre (Mitutoyo, IP65) with precision up to 0.001 mm. Three points of the membrane effective area over 10 membranes were measured and the average thickness calculated.

3 Results and discussion

3.1 Characterisation of the as-synthesized zeolite

Figure 1 shows the XRD pattern of the as-synthesized LTA zeolite with the most critical 2θ reflection peaks at 7.2°, 10.1°, 12.5°, 16.0°, 22°, 23.9°, 27.0°, 30.1° and 34°, in relation with the characteristic peaks reported by Treacy [20]. The sharp peaks of the XRD pattern point to the high crystallinity of the as-synthesized structure. For indexing purposes, the obtained pattern was correlated with the Collection of Simulated XRD Powder Patterns for Zeolites from the Structure Commission of the International Zeolite Association [20] observing the same peaks position but variations in the intensities, perhaps due to preferred orientation or hydration grade. Although, no peaks more than the corresponding to hydrated LTA zeolite structure with a good crystallinity were observed under the synthesis conditions in the as-synthesized dispersed materials

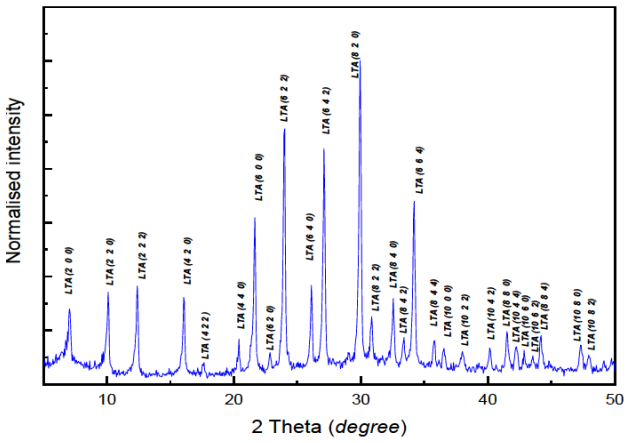

Figure 1: XRD powder diffraction pattern for as-synthesized LTA zeolite under the proposed conditions.

Figure 2 shows the thermal behaviour of the LTA zeolite powders. The thermogravimetric analysis (TGA) curve depicts the hydration behaviour with a continuous water loss as increasing temperature, with a total weight loss of about 17%. The stronger evidence of water loss as the heating processes take place between 40°C and 100°C is associated with the water desorption from the surface of grains in the powdered sample. In the range from 100°C to 200°C are in connections with the external, loosely bound zeolite water [21].

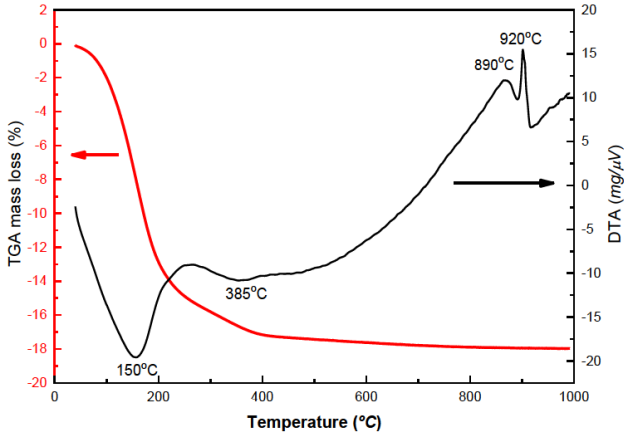

Figure 2: TGA plots of per cent mass loss and DTA for LTA zeolite powders synthesized showing the change in the zeolite structure as a function of temperature.

The losses at higher temperatures are related to the slow desorption of water from the more tightly bound zeolite water molecules in the sodalite cages [22]. These results are correlated with the differential thermal analysis (DTA) curves that first shows an endothermic peak at 150°C attributed to initial desorption of physisorbed water with the initial formation of the anhydrous phase at this temperature. The endothermic behaviour at 385°C in DTA curve corresponds to trapped water molecules in the mentioned cages. With the temperature increase around 500°C and above the TGA, the curve shows a slight mass loss with a tendency to stabilise around 700°C, indicating the completion of the dehydration process. Above this temperature, the Na-LTA framework starts to collapse. No further weight loss up to 800°C is observed. Two exothermic peaks observed in the DTA curve over 800°C are correlated with the structural breakdown of LTA zeolite and the phase transformation to another structure. Szostak [23] associated this fact with the formation of cristobalite or low crystalline carnegiete which structure is based on cristobalite type-structure [24], then thermal stability is limited as much up to 750°C.

To discuss the Fourier transform infrared (FTIR) spectroscopy spectra of samples shown in Figure 3 and the bands assigned for the structure of LTA zeolite was considered the most reported point of view [25–28], which is based on the interpretation of the theoretical spectra corresponding to the vibrations of the D4R structural units in synthetic LTA zeolite [26]. The Figure 3 shows characteristic bands of as-synthesized LTA zeolite in the range 4000 to 400cm^{-1} from the absorption of defined frequencies of these zeolites. The 3430 cm^{-1} bands are close to the typical band 3400 cm^{-1} assigned to the stretching of H bridges attributed to the interaction that occurs in the zeolite cavities by physically adsorbed water by the solid and surface oxygen [22, 23, 25–27]. Vibrations around 1650 cm^{-1} are attributed to the bending of the OH group in adsorbed water [22, 29]. Vibrations reflected at 1000 cm^{-1} are assigned to the asymmetric stretching vibrations characteristic of ν_{as} Si–O (Si) and ν_{as} Si-O (Al) bridge bonds in TO_4 tetrahedra belonging to aluminosilicates with zeolite or sodalite structure [23, 24, 26]. The 662 cm^{-1} bands are assigned to the symmetrical stretching vibrations of the ν_s Si-O-Al bond bridges. The vibrations observed at 560 cm^{-1} are corresponding to a complex band because of the superposition of different bands. The symmetrical stretching vibrations of the ν_s Si - O – Si and the bending vibrations corresponding to δ O - Si – O compose it. The deformation vibrations cause weak bands between 500 and 400 cm^{-1} bands. The vibrations in the 460 cm^{-1} band are correlated to the bending vibrations manifested in antiphase for the δ O-Si-O that is characteristic vibrations belonged to the 4-membered rings [25, 28]. The results in the mid-infrared region are consistent with the XRD study, confirming the LTA zeolite synthesis results.

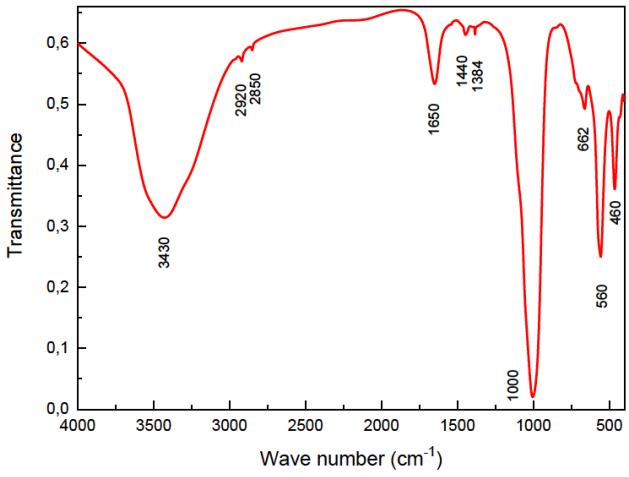

Figure 3: FTIR spectra of the as-synthesized LTA zeolite powders.

SEM image of LTA zeolite powders in Figure 4 shows the crystallisation habits of the as-synthesized zeolite dispersed material with complete and precise crystal particles, focusing on a big crystal. In general, the sample consists of particles aggregates and isolated ones with well-developed faces and defined edges showing cubic and in some cases cubic-octahedral shapes. The crystal shape observed is consistent with the assigned space group *Fm*3*c* for LTA zeolite.

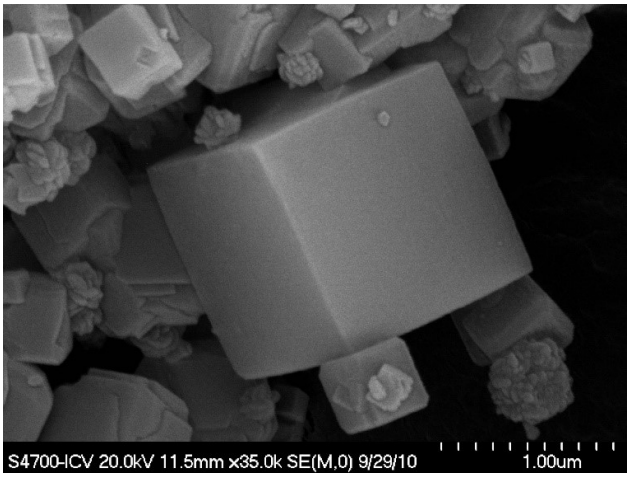

Figure 4: SEM image of LTA zeolite powders showing a large cubic crystal obtained by the hydrothermal method.

Textural properties of the as-synthesized LTA zeolite summarised in Table 1 were evaluated using N_2 and Ar as adsorbate at the temperature of −195.8°C. The value for the surface area according to Brunauer-Emmett-Teller (BET) model using N_2 is relatively low, but also the obtained in the case of Ar, as adsorbate, is comparatively lower than the usual one reported for cation exchanged LTA zeolites [30]. Although it is not frequent, the use of Ar can be justified, not only because the kinetic diameter of the N_2 molecule is comparable with the effective diameter of the zeolite A channel, but also because the presence of a quadrupole moment in N_2 can result in a more significant interaction with the heterogeneous surface of the structure of the zeolite. This fact, in turn, would entail greater difficulty in the differentiation between zeolites of different pore sizes. Besides, if the material were microporous, the adsorption of N_2 in micropores occurs at values of relative pressures lower than Ar adsorption, the latter being more favourable for precise measurements of smaller micropores [31].

Table 1: Textural properties at −195.8°C of as-synthesized LTA zeolite sample using N_2 and Ar as the adsorbate.

Adsorbate	Surface area (m^2/g)	Adsorption cumulative volume of pores (cm^3/g)
N_2	6.6	0.014
Ar	128	0.073

The results in Table 1 can be explained if we consider that the molecules of the adsorbate have had difficulty diffusing through the pores of the Na-LTA zeolite adsorbent. As in the case of the use of N_2 as adsorbate, already mentioned above, attributable not only to the shape of the N_2 molecule but to the presence of Na^+ ions that occupy sites in the cavities and the manifestation of the strong electrostatic field associated with them in the internal surface and its relation to the adsorption properties [32]. Also from the table results, it could be inferred that the difference in the value of the specific surface favourable to the use of Ar as adsorbate, is not determined both by the size of the pores, as by the greater volume of pores to which this adsorbate can access. However, the adsorption of Ar at −195.8°C shows a limited application for the determination of mesoporous size since, under these conditions, the temperature of the system is lower than the corresponding to the triple point [33], showing the following drawbacks:

a) A complete analysis of the micro and mesoporosity is not possible, because, at −195.8°C, the Ar is approximately 6.5 degrees below its triple point,
b) The analysis only makes sense for pore diameters less than 15 nm, because capillary condensation cannot be observed above that pore size.

3.2 Characterisation of mixed matrix membranes

Figure 5 shows the SEM images from the top surface of the *MMMs* with different inorganic fillers weight content: (a) 10% and (b) 20% to the organic solvent methyl-2-pyrrolidinone. Note that zeolite particles (bright spot in the image) are embedded into the polymer and distributed to all over the membrane with good dispersion.

Figure 6 shows cross-section morphology SEM images of the *MMMs* with 20 wt.% and the extent of zeolite particles dispersion within the polymer matrix. The comparison with the previous Figure 5 allows expressing that fillers are also distributed in the volume of the membrane. No apparent voids were observed at the zeolite-polymer interface so, the shaded area around in the vicinity of zeolite agglomerates cannot be estimated or assigned to membrane defects considering the SEM by itself is not enough to elucidate membranes defects and also the stress on the membrane during the manually tear.

The AFM images of the *MMMs* with 20wt.% content is posted in Figure 7, Figure 7a (top view) and 7b (3D view) topography of membrane showing the porous structure of an area of the *MMMs* surface, far from the zeolites, where

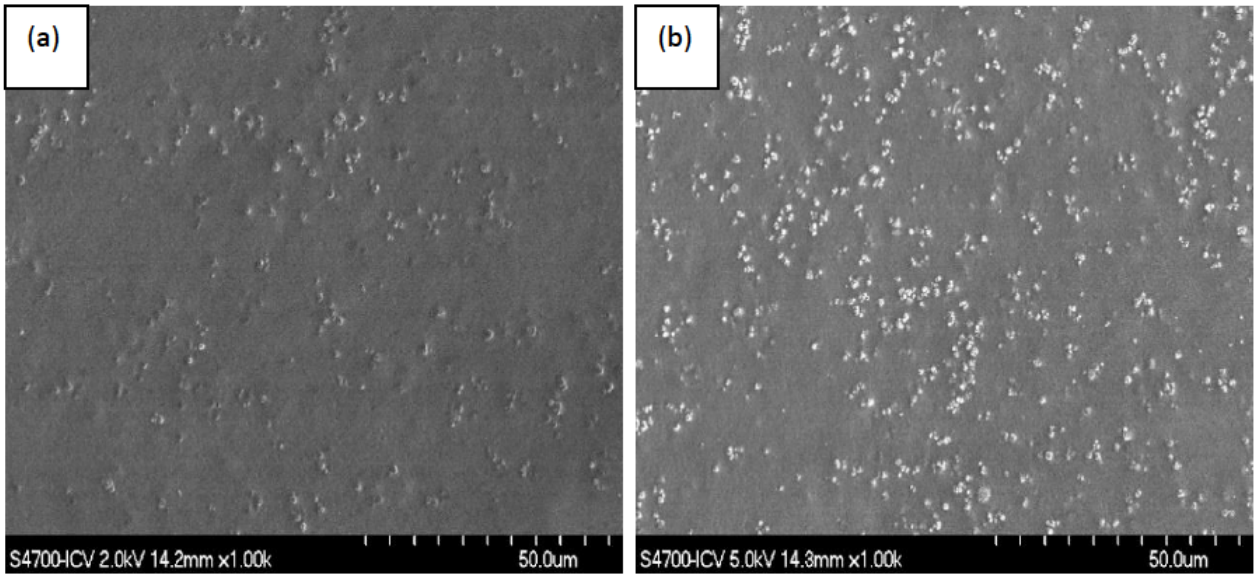

Figure 5: SEM micrographs of *MMMs* with fillers in different weight proportions, (a) 10wt.% and (b) 20wt.% showing the surface morphology.

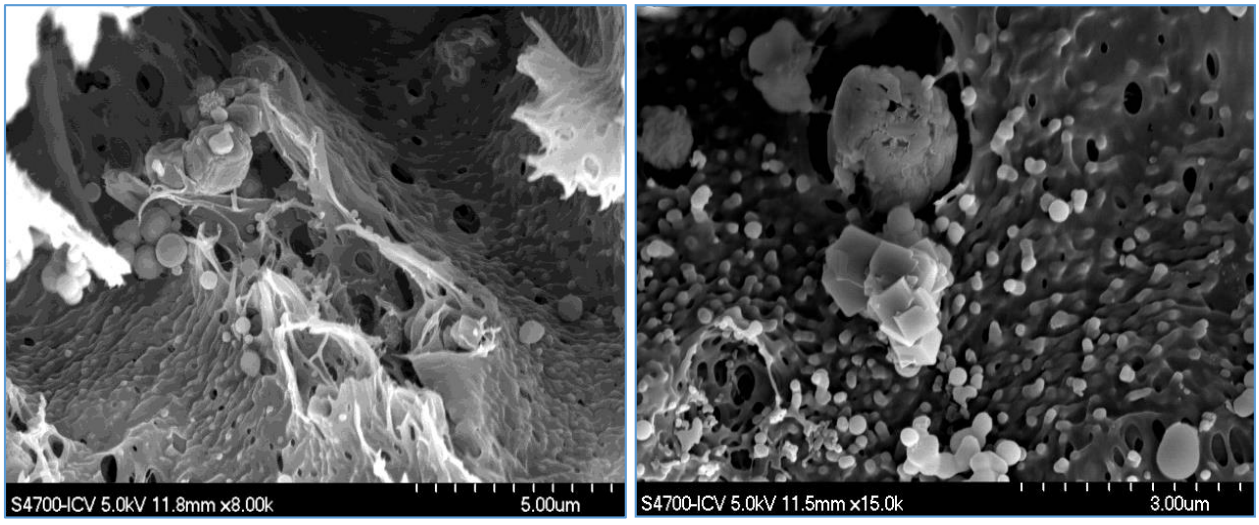

Figure 6: SEM micrographs from the cross-section of the *MMMs* with 20wt.% zeolite fillers showing interfacial morphology.

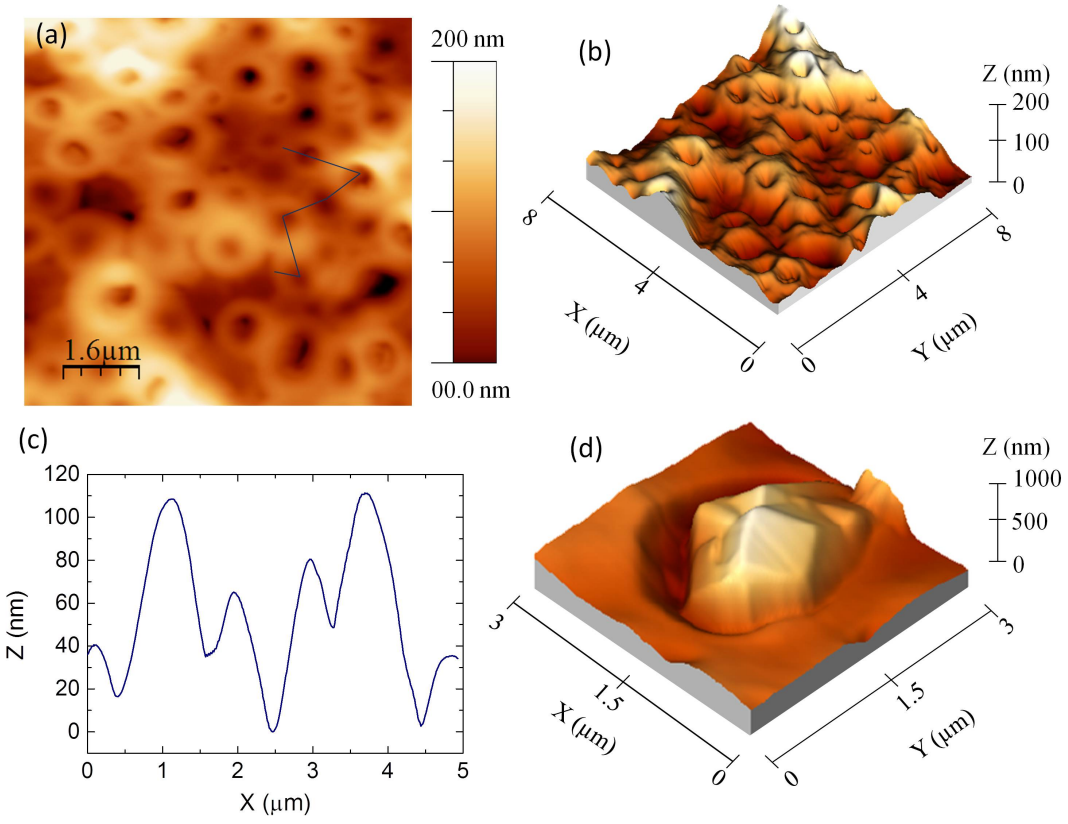

Figure 7: AFM images of *MMMs* surface with a filler content of 20% wt. In Figure 7 (a), the corresponding height scale is included as colour bar.

the dark spots on the images are assigned to the membrane pores, and the brightest portions represent the highest parts of the membrane surface. Figure 7c corresponds to the height profile along the black line marked in Figure 7a. It shows the height differences and sizes of the concerned pores. By inspecting the line profile, it is possible to estimate the sizes of the pores with a funnel shape. The average outer diameter value was around and 0.4 µm and 0.5 µm in the membranes with a content of 10% wt and 20% wt respectively. Finally, Figure 7d corresponds to a 3D-view of a cubic zeolite grain embedded in the polymeric matrix. In this work, by increasing the zeolite concentration from 10 wt.% to 20 wt.%, the surface roughness parameter calculated by AFM decrease from 26.3nm to 20.3nm. It is mentioned in several scientific papers that a certain amount of filler in the polymer matrix at least causes a reduction of membrane surface roughness and it depends on factors as the hydrophilic properties of the filler [34, 35]. However, other authors show otherwise concerning the roughness [36, 37]. These results indicate that the addition of LTA zeolite as filler, at least affected the structure of the surface and therefore the mechanism of formation of the *MMMs*.

Figure 8 outlines the behaviour on single N_2 gas flow through the two studied *MMMs* (Polysulfone matrix with different zeolite loading) as a function of the transmembrane pressure difference. Considering Darcy's law [38] when the data points can fit in a straight line, the flow rate is proportional to the transmembrane pressure difference, so there is no presence in these membranes of an ultralow flow rate of N_2 indicating that the *MMMs*, both at 10wt% and 20 wt.% zeolite loading exhibit high permeability. At 20wt.% zeolite loading, the *MMMs* N_2 flow permeability increased 130% over the 10 wt.% loading even when the thickness of the MMMs 20wt.% loading is quite similar to the other one (157 µm vs 154 µm). It is attributed to the increased fractional free volume caused by the filler assuming good compatibility between the permeability in the polymer phase and the molecular sieves, and no induced plastic deformation of polysulfone takes place in the range of the experimental feed gas pressure. Considering the slope of the lines, the permeability is smaller in 10wt.% composition, the *MMMs* with 10wt.% zeolite loading has a smaller pore size and therefore greater selectivity.

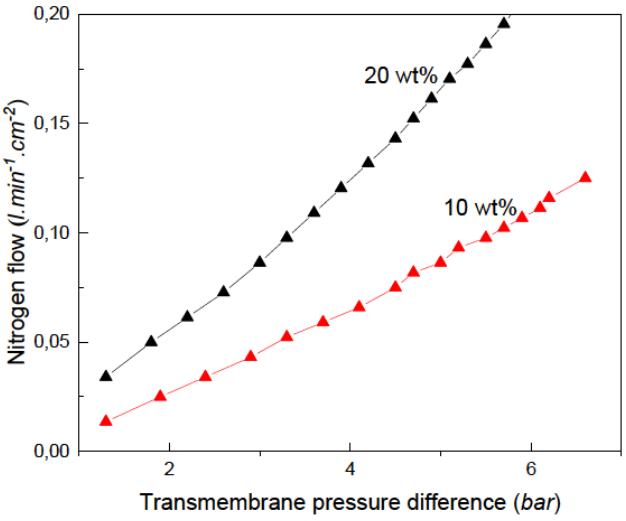

Figure 8: Nitrogen flow through the two studied *MMMs* (Polysulfone matrix with different zeolite loading) as a function of the transmembrane pressure difference.

4 Conclusions

Two specific mixed matrix membranes based on different weight concentrations of zeolite in zeolite/polysulfone composite material (10wt% and 20wt%) with relation to the solvent were synthesised by phase inversion technique.

The main conclusions obtained are:

- The as-synthesized LTA zeolite is characterised by thermal stability up to 750 °C.
- The effect of zeolite concentration modified the surface morphology at least, by altering the surface roughness.
- The increment of molecular sieves loading contributes to the permeability improvement.
- In general, the developed polysulfone/LTA zeolite MMMs can exhibit high permeability and good selectivity.

It is the first step to investigate the feasibility of polysulfone-zeolite based mixed matrix membranes fabricated in our lab facing future approaches to membrane research.

Acknowledgement: The authors gratefully acknowledge the financial support of the Ministry of Economy and Competitiveness of Spain under the projects MAT2013-48426-C2-1R and FIS2017-82415-R; the Ministry of Science, Innovation, and Universities of Spain within the framework of UE M-ERA.NET 2018 program, under the Project Stress LIC. D. F. and acknowledges the Madrid Community support under Project No. PEJD-2017-PRE/IND-4139.

References

[1] Reed TB, Breck DW. Crystalline Zeolite. Crystal Structure of Synthetic Zeolite Type A. J. Am. Chem. Soc. 1956;78(23):5972–7.
[2] Roque-Malherbe R. The Physical Chemistry of Materials: Energy and Environmental Applications. 2nd ed. United Kingdom. CRC Press. Taylor & Francis Group. 2017.
[3] Matsukata M, Kikuchi F. Zeolitic membranes: Synthesis, properties and prospects. Bull Chem Soc Jpn. 1997;70(10):2341–56.
[4] Feng C, Khulbe KC, Matsuura T, Farnood R, Ismail AF. Recent Progress in Zeolite/Zeotype Membranes. Journal of Membrane Science and Research. 2015;(1):49–72.
[5] Fedosov DA, Smirnov AV, Knyzeva EE, Ivanova II. Zeolite Membranes: Synthesis, Properties, and Application. Petrol Chem. 2011;51(8):657–67.
[6] Pera Titus M. Preparation, characterization and modeling of Na zeolite membranes for the pervaporation dehydration of alcohol mixtures. Ph.D. Thesis. Barcelona University; 2006.
[7] Koros WJ. Gas separation membranes: Needs for combined materials science and processing approaches. Polymer Membranes: Structure. Properties and Functions. Wiley. 2002;1(188):13–22.
[8] Khulbe, KC, Feng CY, Matsuura T. Synthetic Polymeric Membranes Characterization by Atomic Force Microscopy. Springer-Verlag Berlin Heidelberg; 2008.
[9] Fang Q, Liu X, Wang N, Ma C, Yang F. The effect of zeolite particle modified by PEG on rubber composite properties. Sci Eng Compos Mater. 2015;22(6):607–12.
[10] Schulze A, Went M, Prager A. Membrane Functionalization with Hyperbranched Polymers. Materials (Basel). 2016 Aug;9(8):706.
[11] Zarshenas K, Raisi A, Aroujalian A. Mixed matrix membrane of nano-zeolite NaX/poly (ether-block-amide) for gas separation applications. J Membr Sci. 2016;510:270–83.
[12] Tai-Shung Chung T, Ying Jianga L, Li Y, Kulprathipanja S. Mixed matrix membranes (MMMs) comprising organic polymers with dispersed inorganic fillers for gas separation. Prog Polym Sci. 2007;32(4):483–507.
[13] Tizchang A, Jafarzadeh Y, Yegani R, Shokri E. Polysulfone nanocomposite membrane embedded by silanized nanodiamond for removal of humic acid from water. J. Water Environ. Nanotechnol. 2019;4(3):213–26.
[14] Souza VC, Quadri MG. Organic-inorganic hybrid membranes in separation processes: a 10-year review. Braz J Chem Eng. 2013;30(04):683–700.
[15] Sanaeepur H, Kargari A, Nasernejad B. Aminosilane-functionalization of a nanoporous Y-type zeolite for application in a cellulose acetate based mixed matrix membrane for CO2 separation. RSC Advances. 2014;4(109):63966–76.
[16] Huang A, Caro J. Facile synthesis of LTA molecular sieve membranes on covalently functionalized supports by using diisocyanates as molecular linkers. J Mater Chem. 2011;21(30):11424–9.
[17] Jacas A, Ortega P, Velasco MJ, Camblor MA, Rodriguez MA. Síntesis de zeolita LTA sobre soportes de corindón: evaluación preliminar para la eliminación de metales pesados de efluentes

acuosos. Bol Soc Esp Ceram Vidr. 2012;51(5):249–54.
[18] Horcas I, Fernández R, Gómez-Rodríguez JM, Colchero J, Gómez-Herrero J, Baro AM. WSXM: a software for scanning probe microscopy and a tool for nanotechnology. Rev Sci Instrum. 2007 Jan;78(1):013705–8.
[19] Conesa A, Fernández A, Pitarch JA, Vicente I, Rodríguez MA. Separation of binary gas mixtures by means of sol–gel modified ceramic membranes. Prediction of membrane performance. J Membr Sci. 1999;155(1):123–31.
[20] Treacy MM, Higgins JB. Collection of simulated XRD Powder Patterns for Zeolites. 5th ed. Elsevier Science; 2007.
[21] Knowlton GD, White TR, McKague HL. Thermal study of types of water associated with clinoptilolite. Clays Clay Miner. 1981;29(5):403–11.
[22] Tounsi H, Mseddi S, Djeme S. Preparation and characterization of Na-LTA zeolite from Tunisian sand and aluminum scrap. Phys Procedia. 2009;2(3):1065–74.
[23] Szostak R. Handbook of Molecular Sieves. New York: Van Nostrand Reinhold; 1992.
[24] Markovic S, Dondur V, Dimitrijevic R. FTIR spectroscopy of framework aluminosilicate structures: carnegieite and pure sodium nepheline. J Mol Struct. 2003;654(1-3):223–34.
[25] Flanigen EM, Khatami H, Szymanski HA. Infrared Structural Studies of Zeolite Frameworks. In: Flanigen EM, Sand LB, editors. Molecular Sieve Zeolites, Advances in Chemistry 101. Washington (DC): American Chemical Society; 1971. pp. 201–29.
[26] Mozgawa W, Jastrzębski W, Handke M. Vibrational spectra of D4R and D6R structural units. J Mol Struct. 2005;744-747:663–70.
[27] Coronas OL, Hernandez MA, Hernandez F, Rojas F, Portillo R, Lara VH, et al. Propiedades de adsorción en zeolitas con anillos de 8 miembros. I. Microporosidad y superficie externa. Revista Matéria. 2009;14(3):918–31.
[28] Mozgawa W, Król M, Barczyk K. FT-IR studies of zeolites from different structural groups. Chemik. 2011;65(7):667–74.
[29] Zhang X, Tang D, Jiang G. Synthesis of zeolite NaA at room temperature: the effect of synthesis parameters on crystal size and its size distribution. Adv Powder Technol. 2013;24(3):689–96.
[30] Sharma P, Song JS, Hee Han M, Hee Cho C. GIS-NaP1 zeolite microspheres as potential water adsorption material: Influence of initial silica concentration on adsorptive and physical/topological properties. Scientific Reports. [Internet]. March 2016; [about 26 p]. Available from https://www.nature.com/articles/srep22734.pdf
[31] Groen JC, Peffer LA, Perez-Ramirez J. Pore size determination in modified micro- and mesoporous materials. Pitfalls and limitations in gas adsorption data analysis. Microporous Mesoporous Mater. 2003;60(1-3):1–17.
[32] Barrer RM. Zeolites and Clay Minerals as Sorbents and Molecular Sieves. London, New York: Academic Press; 1978.
[33] Stork S, Bretinger H, Maier WF. Characterization of micro and mesoporous solids by physisorption methods and pore-size analysis. Appl Catal A Gen. 1998;174(1-2):137–46.
[34] Vatanpour V, Siavash Madaeni S, Rajabi L, Zinadini S, Ashraf Derakhshan A. Boehmite nanoparticles as a new nanofiller for preparation of antifouling mixed matrix membranes. J Membr Sci. 2012;401-402:132–43.
[35] Zinadini S, Zinatizadeh AA, Rahimib M, Vatanpour V, Zangeneh H. Preparation of a novel antifouling mixed matrix PES membrane by embedding graphene oxide nanoplates. J Membr Sci. 2014;453(1):292–301.
[36] Zarshenas K, Raisi A, Aroujalian A. Mixed matrix membrane of nano-zeolite NaX/poly (ether-block-amide) for gas separation applications. J Membr Sci. 2016;510:270–83.
[37] Rezaei M, Ismail AF, Hashemifard SA, Matsuura T. Preparation and characterization of PVDF-montmorillonite mixed matrix hollow fiber membrane for gas-liquid contacting process. Chem Eng Res Des. 2014;92(11):2449–60.
[38] Kuuskraa V. Unconventional Natural Gas. In: Auer P, editor. Advances in Energy System and Technology by Academic Press. Elsevier; 1982. pp. 1–126.